# Title: *In silico* prediction of phosphorylation of NS3 as an essential mechanism for Dengue virus replication and the antiviral activity of Quercetin

**Authors:** Lamya Alomair[1,2], Fahad Almsned[1,3], Aman Ullah[1], and M. Saleet Jafri[1,4*]

**Affiliations:**

[1]School of Systems Biology and the Krasnow Institute for Advanced Study, George Mason University, Fairfax VA 22030, USA

[2]King Abdullah International Medical Research Center, Riyadh, Kingdom of Saudi Arabia

[3]King Fahad Specialist Hospital– Dammam, Dammam, Saudi Arabia.

[4]Center for Biomedical Engineering and Technology, University of Maryland School of Medicine, Baltimore MD 21201, USA

*To whom correspondence should be addressed: sjafri@gmu.edu

**Author Summary:** Dengue is a mosquito-borne virus that infects as many as ~400 million people around the world annually. Dengue causes high fever, severe body aches, rash, and lowered platelet count that could result in Dengue Hemorrhagic Fever. There is currently no cure nor broadly effective vaccine. The interaction of two viral proteins NS3 and NS5 (non-structural proteins 3 and 5) in the infected host's cells is required for viral replication. Our computational modeling studies suggest that phosphorylation of a specific site (S137) of NS3 by

a specific kinase (JNK) increases the interaction of NS3 and NS5, which would enhance viral replication. Experimental studies have shown that inhibition of JNK prevents viral replication. Recent studies have suggested that the plant flavonoid Quercetin, Agathisflavone, and Myricetin inhibit Dengue infection and bind near this phosphorylation site of the viral NS3. Our molecular simulations suggest that these plant flavonoids bind NS3 obstructing phosphorylation of this site which would decrease viral replication. These studies suggest a mechanism and site that can be used to design drugs to treat Dengue.

**Short Title:** Dengue NS3 Phosphorylation

**Abstract**: Infection by Dengue virus is a global health problem for which there have been challenges to obtaining a cure. Current vaccines can only be narrowly applied in ongoing clinical trials. We employed computational methods to predict therapeutic efficacy based on structure-function relationships between human host kinases and viral Nonstructural Protein 3 (NS3) in an effort to understand the therapeutic effect of inhibitors of viral replication. Phosphorylation at each of two most evolutionarily conserved sites, S137 and T189 compared to the unphosphorylated state were studied with molecular dynamics and docking simulations. The simulations suggested that phosphorylation at S137 caused a greater structural change than phosphorylation at T189. Docking studies supported the idea that phosphorylation at S137 increased the binding affinity between NS3 and NS5, whereas, phosphorylation at T189 decreased it. The interaction of NS3 and NS5 is essential for viral replication. Docking studies with the antiviral plant flavonoid Quercetin with NS3 indicated that Quercetin physically occluded the S137 phosphorylation site. Taken together these findings suggest a specific site and mechanism by which Quercetin inhibits Dengue and possible other flaviviruses.

## Introduction

Dengue virus (DENV), also is known as break bone fever, is a serious worldwide health concern afflicting ~400 million individuals in more than 100 countries (1, 2). DENV causes severe illness, and sometimes, a potentially deadly complication called Dengue Hemorrhagic Fever (DHF) (3, 4). The prevalence of Dengue fever has grown dramatically around the world in recent decades, and this global spread of Dengue poses a severe health threat because there are neither specific drugs to treat nor a broadly effective vaccine to prevent the Dengue infection (5-12). Recent studies have suggested that the plant flavonoid Quercetin, Agathisflavone, and

Myricetin inhibit Dengue infection and bind to the same specific site of the viral Nonstructural Protein 3 (NS3) (13, 14). However, the exact mechanism for this inhibition remains unclear. In this study, we performed bioinformatic analysis of the Dengue Proteome to identify amino acid modifications by kinases that are likely to affect viral interaction partners in the human host. We then used molecular simulation to test the functional consequences of phosphorylation at specific sites in NS3. Finally, we determined if the antiviral drug Quercetin was predicted to act at this site.

The DENV genome encodes a polyprotein of 3391 amino acid residues with a gene order of 5′-C-prM-E-NS1-NS2A-NS2B-NS3-NS4A-NS4B-NS5-3′, ten viral proteins including three structural proteins, and seven non-structural (15), The structural proteins are responsible for virion formation, while the nonstructural proteins play roles in the synthesis of viral RNA replication (16). The viral proteins such Nonstructural Protein 3 (NS3) and Nonstructural Protein 5 (NS5) that take part in viral replication and viral protein synthesis enter the host cell and migrate to the endoplasmic reticulum (ER) membrane, which is the site of protein synthesis in the host cell, to use cellular pathways for viral replication (17-19). DENV is a member of the Flaviviridae family that also includes the West Nile virus (WNV) and yellow fever virus, Zika virus and hepatitis C virus (HCV) amongst others and NS3 shares a high degree of homology with other members of this family as shown in the amino acid multiple sequence alignment in Supplemental Fig. S2 (20-24). The relationship of members in this family based on this alignment is shown in Fig. S3.

Both NS3 and NS5 are viral proteins that are vital components in DENV replication. Additionally, NS3 and NS5 contain conserved motifs found in several RNA helicases, and RNA-

dependent RNA polymerases, respectively (25). Phosphorylation of NS5 is critical to its function and association with NS3. Prior research has supported a mechanism where the phosphorylation state of NS5 controls the association/disassociation of NS3 with NS5, which affects viral replication (26). NS3 is the second largest key component in DENV replication machinery. The multifunctional enzyme NS3 performs various actions during viral replication and plays an essential role in antiviral evasion (27). Surprisingly, there is a gap in our understanding of the role of NS3 in molecular mechanisms underlying replication of DENV.

Recently, our lab used a computational approach to predict that NS3 has the potential to be phosphorylated by several of the ~500 human kinases (28). We hypothesized that inhibition of kinases responsible for phosphorylation might inhibit viral replication. We predicted the kinases that are most likely to phosphorylate NS3, by using neural network and other machine learning algorithms to calculate and rank the score of top kinases that phosphorylate DENV NS3 (28). We applied a range of computational methods, including molecular simulations, to classify the functional impact of phosphorylation on NS3 structure on the virus replication on the atomic level. In this paper, we demonstrate, the structural effects caused by NS3 amino acid residue phosphorylation at the two sites S137 and T189, and the impact of these structural effects on NS3 and NS5 interaction, and consequently, on DENV viral replication. NS3 and NS5 are considered to be promising drug targets (22). Finally, we predicted a mechanism behind the anti-viral Quercetin action through its interaction with NS3.

**Materials and Methods**

**Predicting phosphorylation.** To investigate possible amino acids on NS3 that might be phosphorylated by human kinases, we analyzed the NS3 amino acid sequence of by three phospho-algorithms on GPS 3.0 (http://gps.biocuckoo.org/online.php), NetPhos 3.1 (http://www.cbs.dtu.dk/services/NetPhos/), and Scansite 3 (https://scansite4.mit.edu/), which were listed in a recent study as among the most reliable algorithms (29-32). The analyses from these three algorithms revealed many potential candidate phosphorylation sites on NS3 for several kinases. These studies confirmed that phosphoproteins are subject to more conservation in evolution compared to their non-phosphorylated proteins (33, 34). Thus, we carried out *in silico* study combines the results of prediction algorithms with the multiple sequence alignment algorithms, the biological mechanisms, and supports *in vitro* findings from the literature. After that, we prioritize the predicted phosphorylated sites add on our consideration the results from several studies focusing on the conservation of phosphorylated sites and come up with the top kinases.

**System Preparation for Molecular Simulation**

**Initial structure:** We retrieved the initial structure of NS3 from Protein Data Bank (https://www.rcsb.org/structure/2vbc), which is the wild type system, length of 618 amino acids (35, 36). Figure 1 (A) shows the crystallized structure of the NS3 protease-helicase from the dengue virus (PDB 2VBC). The ribbon represents the structure of the alpha-helix, while arrows represent the structure of the beta-sheets were viewed using the Visual Molecular Dynamics viewer (VMD 1.9.3 - https://www.ks.uiuc.edu/Research/vmd/) in new carton graphical representation (37). The domain (N-terminal) of the NS3 (residues 20-168) shown in cyan, the Linker (residues 169-179) shown in blue, and the Helicase Domain (C-terminal) of NS3 (NS3Hel, residues 180-618) shown in pink.

**Phosphorylated structure:** Because phosphorylated SER 137 and THR189 were the focus of our study, we then phosphorylated residues SER 137 and THR189 and created a two phosphorylated system, S137 phosphorylation structure, and T189 Phosphorylated structure using the VMD viewer. The phosphorylated SER137 was modeled using SP2 phosphoserine patch and the THR189 using THP2 phosphothreonine patch. The phosphorylated structures

were saved in the Supplemental files psfgen_phosphorlation137.pgn and psfgen_phosphorlation189.pgn.

**Solvation**: The three systems structures NS3(WT), NS3(S137), NS3(T189) were solvated in a cubic periodic box with TIP3P water model with minimum distance from the protein surface using the VMD viewer (38). With 9517 molecular atoms in the wild type system and 26646, water molecules add the wild type system had 36163 atoms in total. And with 9520 molecular atoms in the phosphorylated protein system and with water molecule add the systems had 36166 atoms in total (Supplementary Fig S1).

**Simulations:** The MD Simulation was prepared and run by Nanoscale Molecular Dynamics (NAMD- https://www.ks.uiuc.edu/Research/namd/) with the CHARMM36 all-force field parameters parallel programming model (39, 40). Periodic boundary condition was used with structures were reported every picosecond (ps). We used a 12 Å cutoff for Van Der Waals interaction with a switching function distance of 8 Å, and the smooth particle-mesh Ewald (PME) method was enabled accordingly, Before the MD simulation, all the flowing procedures were applied to all the three systems.

**Minimization:** Each system was energetically minimization to adjust the structure force field and relax possible steric clashes to obtain a low energy starting conformation. To avoid distress total of 2000 steps of Minimization were performed. This used the namd script file 2VBC_wb_equil.namd included in the supplemental material.

**Heating:** The system was heated from 0 to normal physiological conditions 300 K for 300 ps, with the Langevin thermostat applied. The temperature was incremented slowly by 0.001K. This used the namd scrpt file 2VBC_wb_heat.amd included in the supplemental material.

**Equilibration**: The system equilibration was performed to adjust the system density and this stage and equilibrate kinetic and potential energies. Equilibration stage run under NPT condition for 200 ps. This used the namd scrpt file 2VBC_wb_min.namd included in the supplemental material.

**Simulation:** The three systems were then MD simulated to sample the structural characteristics and dynamics at 300K using NVE ensemble for ten ns under NPT and with time step 1 fs. The long-range electrostatics was handled with the particle-mesh Ewald (PME) methods (41)[29]. The atom coordinate was recorded very one ps throughout the simulation. Additionally, one fs integration step was used for all simulation, then simulated in multiples of 10 ns and 20 ns. This used the namd script file 2VBC_wb_quench.namd included in the supplemental material

**Docking:** The 3D structures of interacting proteins can provide valuable residue and atomic level information regarding the details of the protein-protein interface. It is important for our approach to evaluate the docked conformation interacting proteins NS3(WT), NS3(S137), NS3(T189) and NS5. A protein-protein docking algorithm ClusPro 2.0 server (https://cluspro.bu.edu/) was selected (42-44). ClusPro is an automated and fast rigid-body docking and discrimination algorithm that rapidly filters docked conformations and ranks the conformations using clustering of computed pairwise RMSD values. The docking procedures for predicting protein-protein interactions started with coordinates of Wile Type at the time ten ns docked with NS5. This was followed by the coordinates of the phosphorylated S137 docked with NS5 and finally the with coordinates of phosphorylated T189 docked with NS5 (PDB:2J7U).

**Results**

In this study we performed *in silico* study that combining computational methods, starting with phospho-algorithms on GPS 3.0, NetPhos3.1, and Scansite3, Then we performed Molecular Dynamics (MD) simulation as a computational method for studying the physical movement of atoms and molecules insight into the complex structure of proteins (45, 46)**.** MD lately it has been a predictive method that applied mostly in chemical physics, material science and modeling of biomolecules atomic scales toward a new approach of studying the structural changes induced by phosphorylation and their impact on the protein (47). After that, we used the protein-protein docking algorithm available at ClusPro 2.0 web server (https://cluspro.bu.edu/) to check how phosphorylation on NS3 affected the NS3 and NS5 interaction.

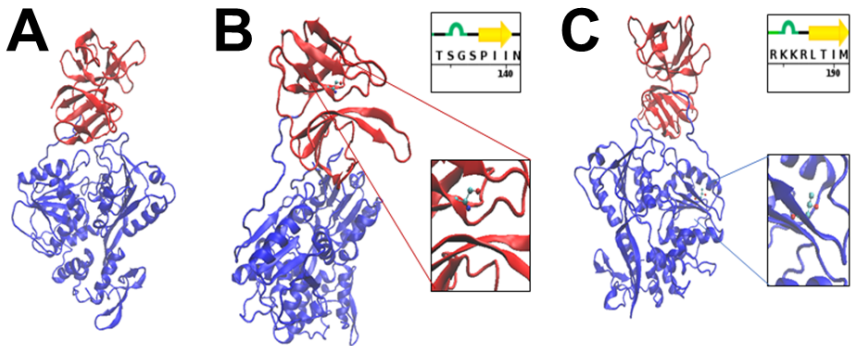


**Fig. 1. NS3 crystal structure. (A)** Crystal structure of the NS3 Protease-Helicase from Dengue Virus (PDB entry 2VBC). The domain (N-terminal) of the NS3 (residues 20-168) shown in red, and the Helicase Domain (C-terminal) of NS3 (NS3Hel, residues 180-618) shown in blue. **(B)** Structure of DENV NS3 (PDB 2VBC) showing the SER 137 residue. On the right, the specific

residue (secondary and tertiary) where phosphorylation can occur is given in a magnified view. On the left, its position within the 3D NS3 structure is shown. **(C)** Structure of DENV NS3 (PDB 2VBC) showing the THR 189 residue. On the right, the specific residue (secondary and tertiary) where phosphorylation can occur is given in a magnified view. On the left, its position within the 3D NS3 structure is shown.

---

The docking of Quercetin (PubChem Database CID=5280343) was performed, against the protease part of the Dengue virus -NS3 protease-helicase (PDB: 2VBC) by using Autodock- Vina (48). The Python scripts in PyRx Virtual Screening software package were used to analyze the docking results (49). UCSF Chimera 1.14 (https://www.cgl.ucsf.edu/chimera/) has been used interactive visualization and analysis of molecular structures (50).

*Phosphorylation prediction*

A computational approach was used to identify phosphorylation sites in the Dengue viral proteins to better understand how the virus might leverage host mechanisms during viral infection and replication. The investigation of possible protein phosphorylation sites revealed many potential candidate positions on DENV NS3, as well as several corresponding human kinases in all three algorithms, GPS 3.0, NetPhos3.1, and Scansite 3, along with their score and residue position in the sequence. Identifying the top kinases required a three-tiered approach. In the first tier, we used our selected tools and predicted a total of 1489, 953, and 108 possible

phosphorylation sites with the associated phosphorylating kinases, respectively. These are all the predictions regardless of redundancy since there are many residues and each can be phosphorylated by more than one kinase. In the second tier, we considered the predicted kinases that have a combination of a high score along with a hit in each of the three tools. The number of kinases decreased to 61, 76, and 64, respectively, from the three tools listed above. Lastly, in the third tier, we took the top 20 kinases from the second tier. Evolutionarily, phosphoproteins are subject to more sequence conservation compared to their non-phosphorylated counterparts (33, 34). Therefore, Multiple Sequence Alignment was applied to identify the most conserved regions among NS3 dengue virus sequences.

The top two candidate phosphorylation sites on NS3 are residue Serine (SER 137 S) which was predicted to be phosphorylated by MAPK, GSK3, CDK1, or JNK2 located on the N-terminal and the residue Threonine (THR 189 T), which was predicted to be phosphorylated by Kinase AKT, PKB(AKT), or CAMK2G, located on the C-terminal, respectively. NS3 is comprised of a N-terminal protease domain (residues 1-168) and a C-terminal (residues 180-618) helicase domain. Both domains have been reported to have enzymatic activity and to be involved in NS3-NS5 interaction (51, 52). To gain insight into the role of phosphorylation at both domains, we examined the structural effects of phosphorylating one amino acid residue from each domain. A graphical representation of DENV NS3 (2VBC) and the SER 137 residue and THR 189 residue is presented in Fig 1.

*Effects of NS3 phosphorylation and conformational change in protein structure*

NS3 is composed of two domains, the protease domain (N-terminal) residues 1-168, and the helicase Domain (C-terminal) residues 180-618. Both the N-terminal protease and C-terminal helicase domains of NS3 are required for its association with NS5 (51). In this study, we examined the phosphorylation of a single site from each domain in NS3, SER137, and THR189 using molecular dynamics simulation. The expectation is that phosphorylation of a functional phosphorylation site should cause a change in protein structure compared to the unphosphorylated structure.

Molecular dynamics simulation of the three systems (un-phosphorylated, phosphorylated S137, phosphorylated T189), were performed for 10 ns using NAMD at 300 K. periodic boundary conditions were used with structures reported every 1 ps, in order to study the structural effects of the phosphorylation on NS3 structures. The root means square devotion (RMSD) and root mean square fluctuation (RMSF) were calculated for all trajectory structure, using R package Bio3D to identify differences in the overall binding structure (53, 54). Also, we plotted the Ψ and Φ angles of the final structure in each simulation. Finally, we conducted hierarchical clustering for the final structure in each simulation using scaled Ψ and Φ values.

One of the ways to represent dihedral angles in proteins is the use of a Ramachandran Plot, We started with a measured Ramachandran plot and marginal density plot of Ψ/Φ angles of four PDB structures files: 1) unphosphorylated system at time 0 ns, 2) unphosphorylated system at time 10 ns, 3) S137 at time 10 ns, 4) T189 at time 10 ns, (Fig. 2A). unphosphorylated system at time 0 ns, unphosphorylated system at time 10 ns, and T189 at time 10 ns showed a close pattern in the plot suggesting that both unphosphorylated system at time 10 ns and T189 at time 10 ns preserved the overall structure of the original protein (unphosphorylated system at time 0).

S137 at time 10 ns (blue dots) showed a greater degree of flexibility by moving toward the right-hand α helix more than the other structures, suggesting a conformational change compared to the original protein (unphosphorylated system at time 0). Furthermore, the hierarchical clustering results for both the Ψ/Φ angles showed the tendency of WT at time 0, WT at time 10 ns, and T189 at time 10 ns and S137 at time 10 ns, cluster together suggesting a change in both angles values compared to the original structure. in Fig. 2B for the Φ angle showed a more significant shift for S137. In Fig. 2C, the Ψ angel also showed a more significant shift for S137.

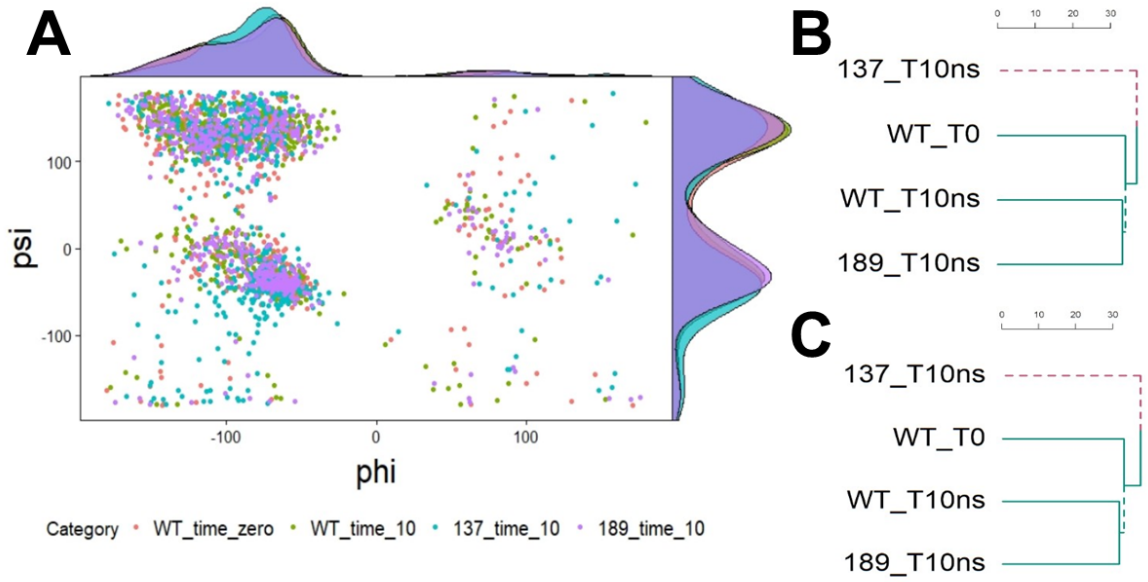


**Fig. 2. Ramachandran plot of NS3 backbone angles. (A)** Plot of the Changes in Ramachandran backbone angles for the 20 ns trajectory and Histogram data for Ψ and Φ is. The backbone torsion angles for the unphosphorylated at time 0 (pink), unphosphorylated at time 20

ns(green), Phosphorylated S137 (blue), Phosphorylated T189 (purple), the Ψ /Φ angles. **(B)** Clustering of Φ angle for the three systems **(C)** clustering of Ψ angle for the three systems.

Calculating the RMSD (root mean squared distance) for the three structures for protein backbone atoms compared to the wild type crystal structure were performed to measure the structure stability of protein inside a solvent box. The RMSD plots were generated based on parameters that were set for the MD simulation (see Materials and Methods), The unphosphorylated system's RMSD plot was compared with the S137, and T189 systems see Fig. 3. In all the 10 ns simulations, the initial crystal structure is given at time 0 ns; then the trajectories relax to stable conformations. At time 10 ns the result shows that the RMSD for S137 and T189 is increased compared to the unphosphorylated system, for example, the intermediate microstates have RMSD between 3-3.5 Å for the unphosphorylated system and between 4-5 Å for the phosphoS137 and phosphoT189. The highest RMSD was observed in S137

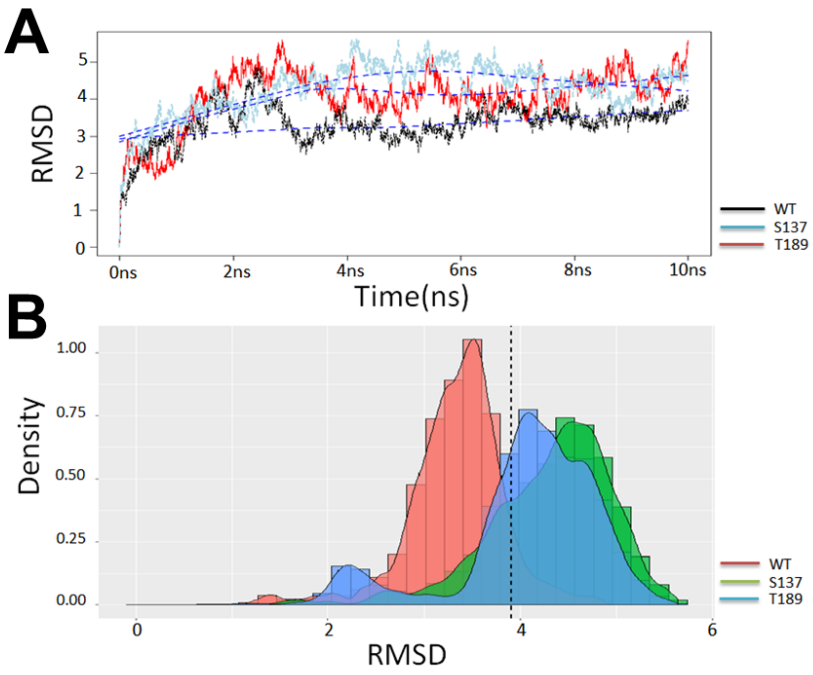


**Fig. 3. RMSD between crystal structure of NS3.** The root mean squared difference from the crystal structure is highest with phosphorylation at S137. **(A)** Conformational changes, RMSD plot of NS3 WT system (black), S137 phosphorylation system showed in (blue) and T189 phosphorylation system (red). **(B)** RMSD Histogram for NS3 WT system (black), RMSD Histogram for NS3 S137 phosphorylation system(green), RMSD Histogram for NS3 T189 phosphorylation system(blue).

phosphorylation where microstates with RMSD >= 5.5 Å and T189. Moreover, Fig 3B the shows that the RMSD Histogram for NS3 S137 phosphorylation system (green) is shifted more than the RMSD Histogram for NS3 T189 phosphorylation system (blue). The RMSD Histogram for NS3 WT system (red) is also shifted from the unphosphorylated crystal structure to a much smaller degree.

*Protein movement changes with phosphorylation*

Calculating the root mean square fluctuation (RMSF) for each residue of the backbone atoms of NS3, unphosphorylated system, and the two phosphorylated S137, T189 systems measures the mobility of the protein residues. Fig. 4A shows that there are slightly larger fluctuations of residues occurring mainly in the phosphorylated NS3 S137 and T189 systems. The RMSF results show the fluctuations regions are at of both the protease and helicase domains of NS3. Fig. 4B shows that the large fluctuation occurs mainly between (residues 49–95), (566-588) have a slightly higher score in S137, which is consistent with earlier work by other on the active site for NS3, which show high mobility during MD simulation (55).

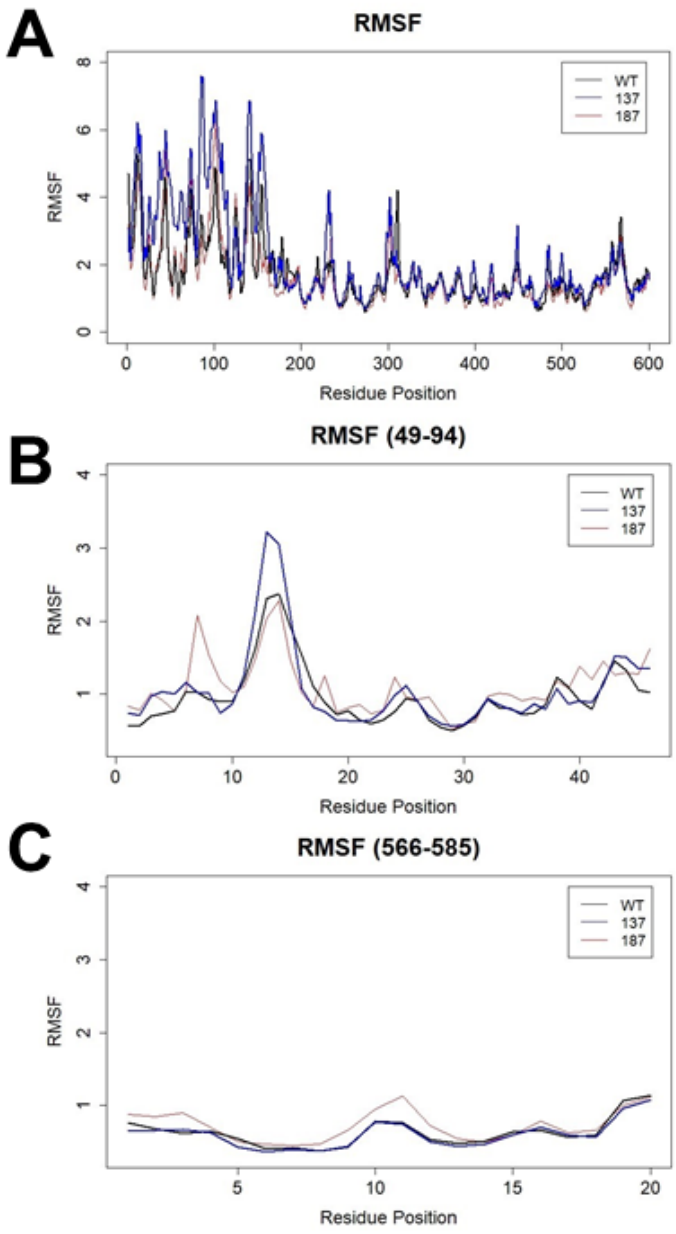


**Fig. 4. RMSF of NS3.** Phosphorylation at S137 increases fluctuations in protein structure in certain regions. (A**)** The RMSF of the residue of NS3 - unphosphorylated (UP - black), S137 (blue)and T189 (Red). (B) The fluctuations in regions (residues 49–95) Unphosphorylated (UP - black), S137(Red)and T189 (blue), **(C)** the fluctuations in regions (566-588) unphosphorylated (UP - black), S137 (red) and T189 (blue).

*Hydrophobicity of the NS3-NS5 contact site increases with phosphorylation*

The solvent accessible surface area (SASA) of unphosphorylated (UP) and phosphorylated NS3 (S137, T189) was calculated for the molecular dynamics' trajectory at time 0 ns and for time 10 ns. SASA is typically calculated by method to account for the free surface area of water molecules within a radius of 1.4 Å. Simulated structures show that several residues on the (S137, T189) have larger SASA than that of the unphosphorylated system. The larger the SASA of residue is, the more hydrophilic the residue, suggesting that the atoms are exposed more to water. Conversely, increasing the hydrophobicity of a residue may facilitate NS3 interaction with other molecules, such as NS5, or a protein kinase. Fig. 5A shows the SASA calculated for all residue at time 10 ns for the unphosphorylated system (UP - blue) and S137 (S137 red). The S137 system residues (red) have larger SASA scores, indicating that residues on the S137 had larger SASA than that of the unphosphorylated system. Fig, 5B shows that residues 566-585 in the phosphorylated state produces a larger SASA than the unphosphorylated state. These results are consistent with the observations in MD trajectories RMSD and RMSF and which is consistent with earlier work of the active site for NS3 and which we showed to be important for NS3-NS5 interaction [44].

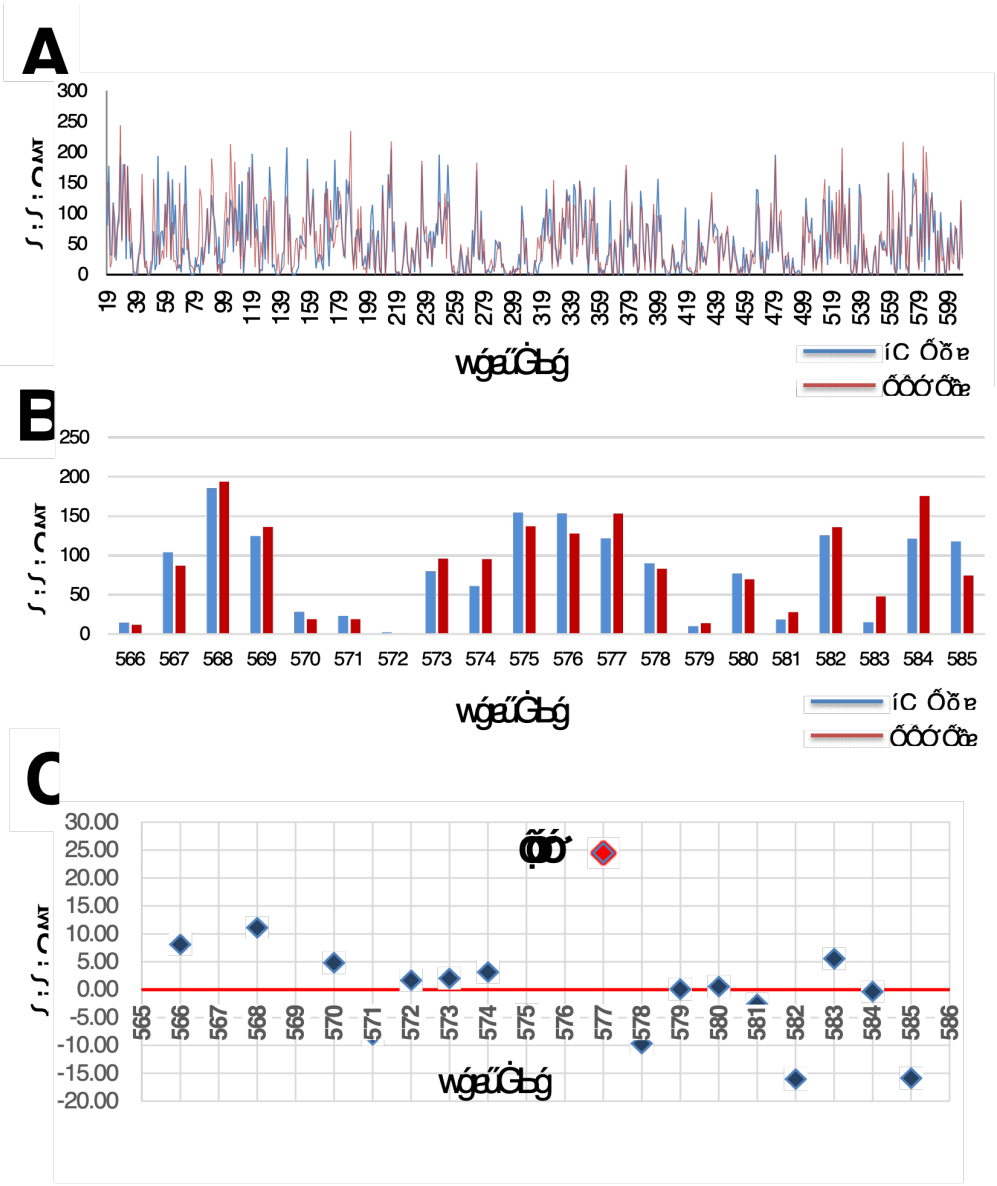


**Fig 5. Solvent accessible surface area of NS3.** Phosphorylation of S137 increases the solvent accessibility at many of the residues in the C-terminal end of NS3 making it more available for interaction with NS5. **A.** All Residue SASA at time 10 ns (unphosphorylated blue, S137 red). **B.** SASA for residue (566-585) at time 10 ns wild type blue and S137 orange. **C**. Plot of the difference in Solvent-Accessible Surface Area score between (WT and 137) in the zoom we can see that 577(red) SASA is increased.

*Phosphorylation-induced site-specific structural changes*

Detection of increased negative-strand RNA synthesis by real time RT-PCR for the NS3:N570A mutant suggests that NS3-NS5 interaction plays an important role in the balanced synthesis of positive- and negative-strand RNA for robust viral replication (55). In particular, the 50 C-terminal amino acid residues are important for this interaction. Simulations suggest that the phosphorylation of residues S137 in NS3 might disrupt the NS3-NS5 interaction through

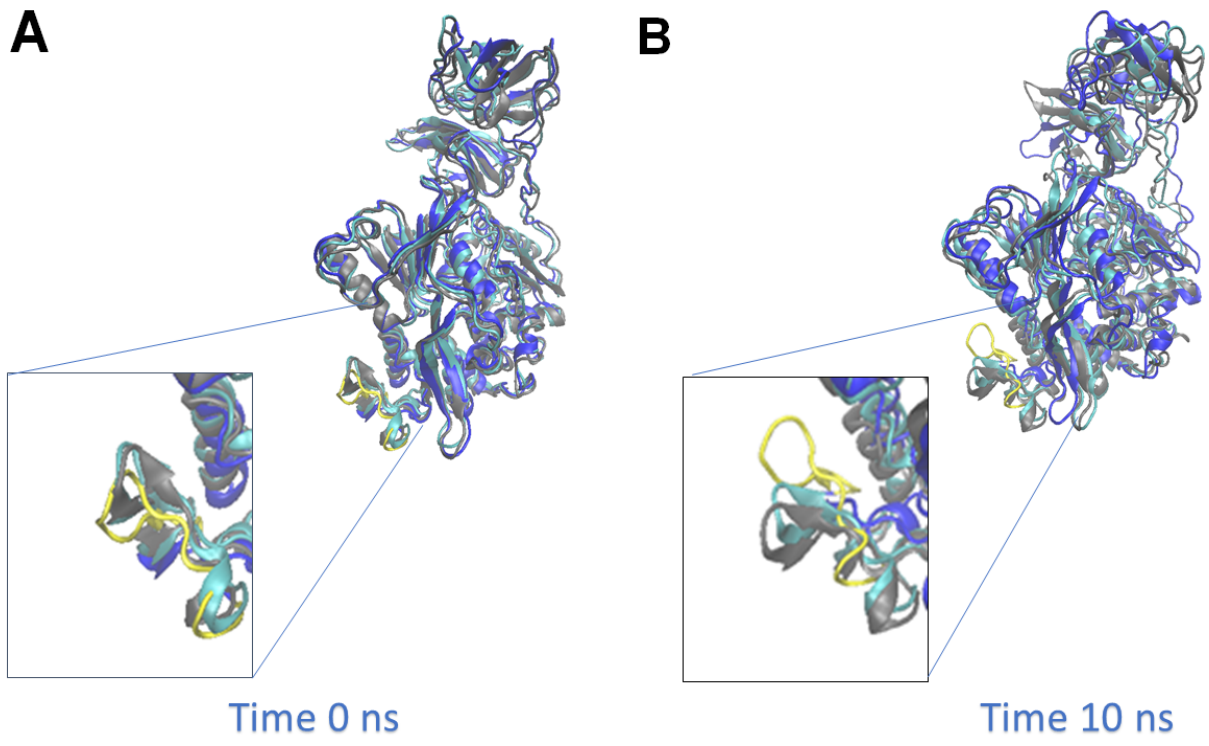


**Fig. 6. Site specific changes in NS3 structure with phosphorylation.** The C-terminal amino acid residues are important for the interaction of NS3 with NS5. The crystal structure shows the

residue 577 highlighted in yellow. **A.** Simulated structure at time 0 (UP green, S137 blue, T189 gray). **B.** Simulated structure at time 10 at 3 system (WT green, S137 blue, T189 gray) changes in the structure at residues 566–585. The effect of the phosphorylation after 10 ns of simulation is shown in Fig. 6. The structure of the unphosphorylated system (green)and S137 (blue) and 189 (gray) show that the residue 577 at time 0 and at time 10 ns differ in position with residue 577 being in a more exposed loop (highlighted in yellow).

*Docking Analysis of NS3-NS5 Interaction*

To simulate the effect of the phosphorylation of NS3 structures on the NS3-NS5 interaction, ClusPro web server has been used to perform a blind protein-protein docking between (NS5) and the final structure in each. Docking was used to explore the interactions between NS3 Wild type, NS3 S137, NS3 T189 with NS5. Blind protein-protein docking between NS5 and the final structure in each MD simulation (WT, S137, T189) using the ClusPro web server has been conducted to predict the three-dimensional structures of the macromolecular complexes that are most likely to occur in nature. The lowest energy as determined by using the thermodynamic stabilities were calculated using the ClusPro formula for Coefficient Weights

$$E = 0.40Erep + -0.40Eatt + 600Eelec + 1.00EDARS$$

| ID | |
|---|---|
| WT | -1045.0 Kcal/mol |
| 189 | -960.8 Kcal/mol |
| 137 | -1204.2 Kcal/mol |

**Table 1. NS3-NS5 docking energies.** Docking results obtained from ClusPro Server (blind docking with NS5) show that phosphorylation at S137 created the most stable NS3-NS5 binding pair.

The balanced form of the equation has been used to choose the candidates posing and to assess the stability of the interaction between NS3 and NS5. Based on ClusPro results, the S137-NS5 complex had the lowest docking energy compared to the T187 and the unphosphorylated structures. Table 1 shows the binding free energy. The non-phosphorylated (S137, T189) and phosphorylated are all negative values, indicating that these complexes were energetically favorable. Phosphorylated S137 (-1204.2 Kcal/mol) was lower in energy than the non-phosphorylated (-1045.0 Kcal/mol). On the other hand, phosphorylation at T189 decreased the binding affinity. This result suggests that the NS3 S137 has lower binding energy indicating that the NS3-NS5 interaction is more stable. This result suggests phosphorylation of residue Serine (SER 137 S) which this study predicted to be phosphorylated with MAPK, GSK3, CDK1, JNK2 is likely to stabilize the NS3-NS5 interaction. The disruption of NS3-NS5 interaction results in the transport of NS5 to the nucleus which decreases viral replication suggesting that S137 phosphorylation aids in Dengue (and flavivirus replication) [11]. Among the MAPKs, there are the JNK and p38 kinases, whose pathways are activated during DENV infection in macrophages. Previous experimental studies have found that phosphorylation by JNK, ERK1/2, and P38 MAPK is activated during Dengue infection and that the inhibitors of JNK and p38 pathways reduce the viral activity (56, 57).

*Interactions of NS3 with Quercetin*

Quercetin is a plant flavonoid that experimentally inhibits Dengue replication and binds to NS3. In fact, among the associated antiviral activities, the flavonoid Quercetin has been reported to

significantly reduce dengue DENV serotype 2 levels by 67% (58). Studies have measured the binding kinetics of Quercetin to NS3 estimating a $K_D$ of 20 µM (14). Computational studies using molecular docking strongly suggested the binding site of Quercetin to NS2B-NS3, however, the mechanism of viral inhibition is still unknown (13, 14).

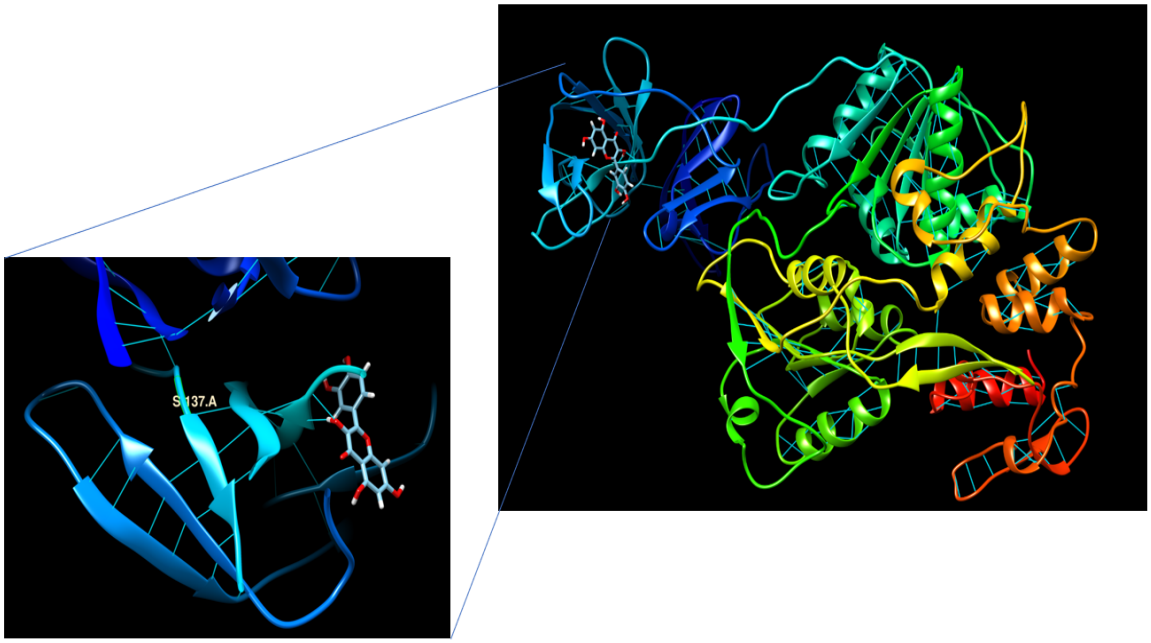


**Fig. 7. Docking of Quercetin with NS3.** Auto-dock of Quercetin against the protease part of the Dengue virus shows that Quercetin binds very close to the S137 site occluding its access.

Auto-dock Vina yielded 10 poses of Quercetin against the protease part of the Dengue virus -NS3 protease-helicase. The site of docking is similar to those found in previous studies (13, 14). The binding free energy of these poses are ranging from -6.6 to -7.4 kcal/mol. the pose with the lowest energy is shown in Fig. 8. Hydrogen bonds have been added to Dengue virus NS3 protease-helicase before and after Quercetin docking. two hydrogen bonds are connecting Quercetin to the protease part of the Dengue virus, one bond with GLN 167 A and THR 166A.

donated from oxygen atom (O5). The position of the quercetin physically occludes access to S137 suggesting a possible mechanism where quercetin blocks the phosphorylation of NS3 at 137. This keeps the binding affinity between NS3 and NS5 at a lower level allowing their dissociation which interferes with viral replication.

**Discussion**

A better understanding of the role of individual viral proteins and how they interact with human host proteins is needed to in order to develop effective drug treatments for Dengue. Association of NS3 and NS5 in the cytoplasm is required for Dengue virus replication. Experimental studies have shown that phosphorylation of NS5 results its dissociation and translocation to the nucleus (26, 59). One of these studies specifically found that protein kinase C (PKC) mediated phosphorylation was critical for this process. With this in mind, this study explored how phosphorylation of NS3 affected the association of NS3 and NS5. Of the many potential phosphorylation sites found using prediction software, the two most conserved S137 and T189 were explored. Molecular dynamics studies demonstrated that phosphorylation at S137 causes a larger structural change in NS3 compared to the unphosphorylated system than phosphorylation at T189. Furthermore, docking studies showed that phosphorylation at S137 increased the binding affinity between NS3 and NS5. In contrast, phosphorylation at T189 lowers the binding affinity. Phosphorylation at S 137 was predicted for MAPK, GSK3, CDK1, and JNK2. Experimental studies have shown that activation of JNK enhances Dengue infection, supporting this prediction (56, 57).

The domain containing S137 is an important functionally conserved region in the flavivirus family (24). Protein homology models have suggested that this residue is involved in the "catalytic triad" (His-Asp-Ser135) that is conserved in all flaviviruses and is necessary for viral replication (24). Site directed mutagenesis at this site, converting Ser to and Ala at residue 135 in yellow fever virus (equivalent to S137 in Dengue virus) abolished replication (60). Computational studies have explored the catalytic triad as a drug target in screens for potential substrates (3, 61-64). However, these studies could not link a potential drug candidate to an experimentally observed reduction in viral replication (61-64). The proximity of S137 to this critical triad site suggests that its phosphorylation is likely to be functionally important.

Several plant flavonoids have been shown to display antiviral activity against viruses in the flavivirus family which includes the Dengue virus. These include Quercetin, Agathisflavone, and Myricetin which have been shown to bind NS3 at the same site (13, 14). Quercetin binds with the highest affinity with a disassociation constant of 20 μM. Docking simulations performed in the current study predicts that Quercetin binds NS3 so as to occlude access to the S137 phosphorylation site. Quercetin has also has been shown to be an inhibitor of JNK in treating cardiovascular diseases related to vascular smooth muscle cells (VSMC) growth and apoptosis (65). In essences, this provides a molecular target for inhibiting Dengue virus and suggests that these flavonoids are all acting at this site. Our *in silico* findings sets up future experimental studies to explore this hypothesis and should advance current understanding of Dengue infection and may provide ways to inhibit viral replication. In addition, future studies will include experimental verification that flavonoids such as Quercetin act at this site to prevent phosphorylation at residue S137. Quercetin is predicted to bind this site with insufficient affinity

to be a suitable drug. Therefore, other compounds that bind this site would need to be found. Such studies would be followed by optimization of lead compounds, possibly similar that are to Quercetin, Agathisflavone, and Myricetin, since having the molecular target and structure would allow a pharmacophore model to be developed.

To our knowledge, this is the first study that examined the structural effects NS3 specific amino acid residue phosphorylation on protein structure and its impact on NS3 and NS5 interaction, and consequently, on DENV viral replication. In summary, the computational analysis and molecular simulations presented in the study make three predictions. First. We predict that phosphorylation of NS3 is important for its replicase activity by strengthening its association with NS5. Second, these studies predict that NS3 is phosphorylated by JNK as the S137 site. Third, Quercetin and other plant flavonoids inhibit viral replication by binding near this site to obstruct access to S137. Fourth, given the high degree of homology of this region of NS3 in the flavivirus family, this presents a potential mechanism that is common across members in this family, except perhaps Hepatitis C virus which lacks S137 (Supplemental Fig S2 and S3). While these predictions are consistent with existing experimental studies, future work is needed to test these hypotheses.

**Acknowledgments:** The authors would like to thank Robert Lipsky and Habib Bokhari for their helpful comments during this work. The authors would like to thank Mohamed A. Hussein, MSCS, MsPH, PhD (Chairman, Department Biostatistics and Bioinformatics, King Abdullah International Medical Research Center National Guard Riyadh Saudi Arabia) for his support. The authors are grateful to Professor Dmitri Klimov (GMU School of Systems Biology USA) for providing initial help with the molecular dynamics simulations.

**Funding**: This work was supported by King Abdullah International Medical Research Center (LA), National Guard Saudi Arabia (FA). This research was supported by National Institutes of Health (NIH) grant no. 5R01HL105239 (MSJ & AU), 5U01HL116321 (MSJ & AU)

**Author contributions**:

LA and SJ start the conceptualization of this work. LA performed and analyzed Molecular dynamics simulations, AU helped with Molecular dynamics simulations, FA helped with analysis and docking. LA wrote the original draft, All authors contributed to the discussion, the analysis of data, and the final draft of the paper.

**Data and materials availability**: Data will be deposited into the Mason Archival Repository Service (MARS) located at http://mars.gmu.edu upon manuscript acceptance.

**Figures**:

**Fig. 1. NS3 crystal structure. (A)** Crystal structure of the NS3 Protease-Helicase from Dengue Virus (PDB entry 2VBC). The domain (N-terminal) of the NS3 (residues 20-168) shown in red, and the Helicase Domain (C-terminal) of NS3 (NS3Hel, residues 180-618) shown in blue. **(B)** Structure of DENV NS3 (PDB 2VBC) showing the SER 137 residue. On the right, the specific residue (secondary and tertiary) where phosphorylation can occur is given in a magnified view. On the left, its position within the 3D NS3 structure is shown. **(C)** Structure of DENV NS3 (PDB 2VBC) showing the THR 189 residue. On the right, the specific residue (secondary and tertiary) where phosphorylation can occur is given in a magnified view. On the left, its position within the 3D NS3 structure is shown.

**Fig. 2. Ramachandran plot of NS3 backbone angles. (A)** Plot of the Changes in Ramachandran backbone angles for the 20 ns trajectory and Histogram data for Ψ and Φ is. The backbone torsion angles for the unphosphorylated at time 0 (pink), unphosphorylated at time 20 ns(green), Phosphorylated S137 (blue), Phosphorylated T189 (purple), the Ψ /Φ angles. **(B)** Clustering of Φ angle for the three systems **(C)** clustering of Ψ angle for the three systems.

**Fig. 3. RMSD between crystal structure of NS3.** The root mean squared difference from the crystal structure is highest with phosphorylation at S137. **(A)** Conformational changes, RMSD plot of NS3 WT system (black), S137 phosphorylation system showed in (blue) and T189 phosphorylation system (red). **(B)** RMSD Histogram for NS3 WT system (black), RMSD

Histogram for NS3 S137 phosphorylation system(green), RMSD Histogram for NS3 T189 phosphorylation system(blue).

**Fig. 4. RMSF of NS3.** Phosphorylation at S137 increases fluctuations in protein structure in certain regions. (A**)** The RMSF of the residue of NS3 - unphosphorylated (UP - black), S137 (blue)and T189 (Red). (B) The fluctuations in regions (residues 49–95) Unphosphorylated (UP - black), S137(Red)and T189 (blue), **(C)** the fluctuations in regions (566-588) unphosphorylated (UP - black), S137 (red) and T189 (blue).

**Fig 5. Solvent accessible surface area of NS3.** Phosphorylation of S137 increases the solvent accessibility at many of the residues in the C-terminal end of NS3 making it more available for interaction with NS5. **A.** All Residue SASA at time 10 ns (unphosphorylated blue, S137 red). **B.** SASA for residue (566-585) at time 10 ns wild type blue and S137 orange. **C**. Plot of the difference in Solvent-Accessible Surface Area score between (WT and 137) in the zoom we can see that 577(red) SASA is increased.

**Fig. 6. Site specific changes in NS3 structure with phosphorylation.** The C-terminal amino acid residues are important for the interaction of NS3 with NS5. The crystal structure shows the residue 577 highlighted in yellow. **A.** Simulated structure at time 0 (UP green, S137 blue, T189 gray). **B.** Simulated structure at time 10 at 3 system (WT green, S137 blue, T189 gray).

**Fig. 7. Docking of Quercetin with NS3.** Auto-dock of Quercetin against the protease part of the Dengue virus shows that Quercetin binds very close to the S137 site occluding its access.

**Table 1. NS3-NS5 docking energies.** Docking results obtained from ClusPro Server (blind docking with NS5) show that phosphorylation at S137 created the most stable NS3-NS5 binding pair.

**Supplementary Materials**

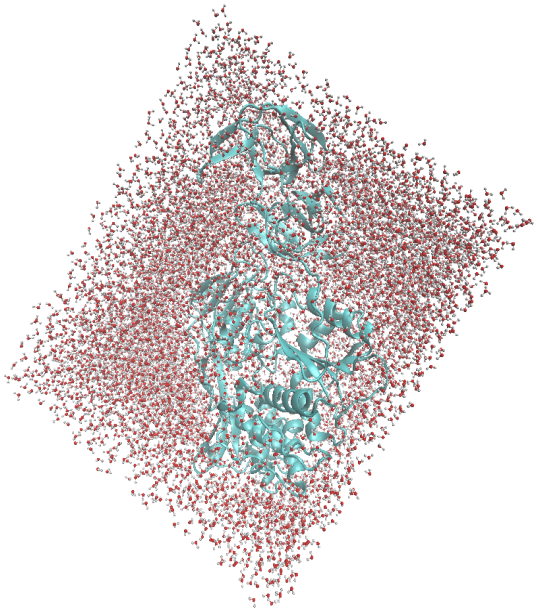

**Fig. S1. Simulation box for molecular simulation of NS3.**

The solvated system of NS3 2vbc Crystal structure the protein solvent with a box of water illustrated by VMD.


**Fig. S2. Multiple sequence Alignment of *Flavivirus* family.**

Dengue virus (all four serotypes), hepatitis C virus, yellow fever virus, zika virus, West Nile virus, Murray Valley encephalitis, and Japanese encephalitis are all members of the *Flavivirus* family. Aura virus, Chikungunya virus and Barmah virus (carried by mosquitoes but not of the *Flavivirus* family) are included for comparison. The *Flavivirus* family show a high degree of homology especially in the regions flanking S137 indicated by the red arrow.

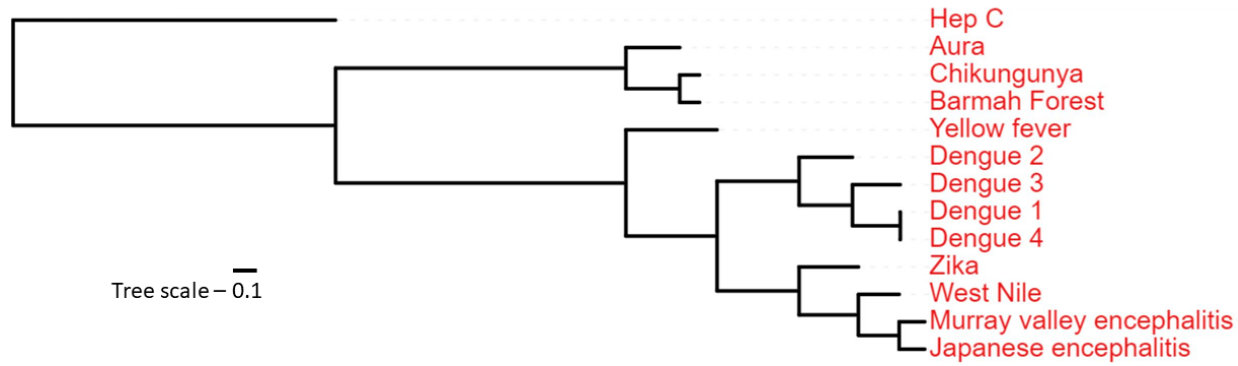


**Fig. S3. Phylogenetic tree for *Flavivirus* family.** Most of the *Flavivirus* family viruses show are very similar with hepatitis C diverging from the rest. The non-*Flavivirus* family viruses cluster separately.

## References


1. Friedrich MJ. Asymptomatic People May Contribute to Dengue TransmissionAsymptomatic People May Contribute to Dengue TransmissionGlobal Health. JAMA. 2016;315(3):242-.
2. Beesetti H, Khanna N, Swaminathan S. Drugs for dengue: a patent review (2010-2014). Expert Opin Ther Pat. 2014;24(11):1171-84.
3. Chan KWK, Watanabe S, Jin JY, Pompon J, Teng D, Alonso S, et al. A T164S mutation in the dengue virus NS1 protein is associated with greater disease severity in mice. Sci Transl Med. 2019;11(498).
4. Murphy BR, Whitehead SS. Immune response to dengue virus and prospects for a vaccine. Annu Rev Immunol. 2011;29:587-619.
5. Brady OJ, Gething PW, Bhatt S, Messina JP, Brownstein JS, Hoen AG, et al. Refining the global spatial limits of dengue virus transmission by evidence-based consensus. PLoS Negl Trop Dis. 2012;6(8):e1760.
6. Gubler DJ. Dengue, Urbanization and Globalization: The Unholy Trinity of the 21(st) Century. Trop Med Health. 2011;39(4 Suppl):3-11.
7. Bidet K, Ho V, Chu CW, Naim ANH, Thazin K, Chan KR, et al. Mimicking immune signatures of flavivirus infection with targeted adjuvants improves dengue subunit vaccine immunogenicity. npj Vaccines. 2019;4(1):3.
8. Messina JP, Brady OJ, Golding N, Kraemer MUG, Wint GRW, Ray SE, et al. The current and future global distribution and population at risk of dengue. Nature Microbiology. 2019.
9. Feinberg MB, Ahmed R. Advancing dengue vaccine development. Science. 2017;358(6365):865-6.
10. Friedrich MJ. Global Temperature Affects DengueGlobal Temperature Affects DengueGlobal Health. JAMA. 2018;320(3):227-.
11. Freedman D, LH C, Kozarsky P. Medical Considerations before International Travel. N Engl J Med. 2016;375:247-60.
12. Robinson ML, Durbin AP. Dengue vaccines: implications for dengue control. Curr Opin Infect Dis. 2017;30(5):449-54.
13. Senthilvel P, Lavanya P, Kumar KM, Swetha R, Anitha P, Bag S, et al. Flavonoid from Carica papaya inhibits NS2B-NS3 protease and prevents Dengue 2 viral assembly. Bioinformation. 2013;9(18):889-95.
14. de Sousa LR, Wu H, Nebo L, Fernandes JB, da Silva MF, Kiefer W, et al. Flavonoids as noncompetitive inhibitors of Dengue virus NS2B-NS3 protease: inhibition kinetics and docking studies. Bioorg Med Chem. 2015;23(3):466-70.
15. Bartholomeusz AI, Wright PJ. Synthesis of dengue virus RNA in vitro: initiation and the involvement of proteins NS3 and NS5. Arch Virol. 1993;128(1-2):111-21.
16. Mukhopadhyay S, Kuhn RJ, Rossmann MG. A structural perspective of the flavivirus life cycle. Nat Rev Microbiol. 2005;3(1):13-22.
17. Limjindaporn T, Wongwiwat W, Noisakran S, Srisawat C, Netsawang J, Puttikhunt C, et al. Interaction of dengue virus envelope protein with endoplasmic reticulum-resident chaperones facilitates dengue virus production. Biochem Biophys Res Commun. 2009;379(2):196-200.
18. Reid DW, Campos RK, Child JR, Zheng T, Chan KWK, Bradrick SS, et al. Dengue Virus Selectively Annexes Endoplasmic Reticulum-Associated Translation Machinery as a Strategy for Co-opting Host Cell Protein Synthesis. J Virol. 2018;92(7).
19. Neufeldt CJ, Cortese M, Acosta EG, Bartenschlager R. Rewiring cellular networks by members of the Flaviviridae family. Nature Reviews Microbiology. 2018;16:125.
20. Kuno G, Chang GJ, Tsuchiya KR, Karabatsos N, Cropp CB. Phylogeny of the genus Flavivirus. J Virol. 1998;72(1):73-83.
21. Wu J, Bera AK, Kuhn RJ, Smith JL. Structure of the Flavivirus helicase: implications for catalytic activity, protein interactions, and proteolytic processing. J Virol. 2005;79(16):10268-77.

22. Luo D, Vasudevan SG, Lescar J. The flavivirus NS2B-NS3 protease-helicase as a target for antiviral drug development. Antiviral Res. 2015;118:148-58.
23. Li Z, Zhang J, Li H. Chapter 7 - Flavivirus NS2B/NS3 Protease: Structure, Function, and Inhibition. In: Gupta S, editor. Viral Proteases and Their Inhibitors: Academic Press; 2017. p. 163-88.
24. Brinkworth RI, Fairlie DP, Leung D, Young PR. Homology model of the dengue 2 virus NS3 protease: putative interactions with both substrate and NS2B cofactor. J Gen Virol. 1999;80 ( Pt 5):1167-77.
25. Papageorgiou L, Loukatou S, Sofia K, Maroulis D, Vlachakis D. An updated evolutionary study of Flaviviridae NS3 helicase and NS5 RNA-dependent RNA polymerase reveals novel invariable motifs as potential pharmacological targets. Mol Biosyst. 2016;12(7):2080-93.
26. Kapoor M, Zhang L, Ramachandra M, Kusukawa J, Ebner KE, Padmanabhan R. Association between NS3 and NS5 proteins of dengue virus type 2 in the putative RNA replicase is linked to differential phosphorylation of NS5. J Biol Chem. 1995;270(32):19100-6.
27. Natarajan S. NS3 protease from flavivirus as a target for designing antiviral inhibitors against dengue virus. Genet Mol Biol. 2010;33(2):214-9.
28. Alomair L. Combining Protein Interactions and Functionality Classification in NS3 to Determine Specific Antiviral Targets in Dengue. United States - Virginia: George Mason University; 2017.
29. Xue Y, Liu Z, Cao J, Ma Q, Gao X, Wang Q, et al. GPS 2.1: enhanced prediction of kinase-specific phosphorylation sites with an algorithm of motif length selection. Protein Eng Des Sel. 2011;24(3):255-60.
30. Blom N, Sicheritz-Ponten T, Gupta R, Gammeltoft S, Brunak S. Prediction of post-translational glycosylation and phosphorylation of proteins from the amino acid sequence. Proteomics. 2004;4(6):1633-49.
31. Obenauer JC, Cantley LC, Yaffe MB. Scansite 2.0: Proteome-wide prediction of cell signaling interactions using short sequence motifs. Nucleic Acids Res. 2003;31(13):3635-41.
32. Vlachakis D, Bencurova E, Papageorgiou L, Bhide M, Kossida S. Protein phosphorylation prediction: limitations, merits and pitfalls. Journal of Molecular Biochemistry. 2015.
33. Boekhorst J, van Breukelen B, Heck A, Jr., Snel B. Comparative phosphoproteomics reveals evolutionary and functional conservation of phosphorylation across eukaryotes. Genome Biol. 2008;9(10):R144.
34. Macek B, Gnad F, Soufi B, Kumar C, Olsen JV, Mijakovic I, et al. Phosphoproteome analysis of E. coli reveals evolutionary conservation of bacterial Ser/Thr/Tyr phosphorylation. Mol Cell Proteomics. 2008;7(2):299-307.
35. Berman HM, Westbrook J, Feng Z, Gilliland G, Bhat TN, Weissig H, et al. The Protein Data Bank. Nucleic Acids Res. 2000;28(1):235-42.
36. Luo D, Xu T, Hunke C, Gruber G, Vasudevan SG, Lescar J. Crystal structure of the NS3 protease-helicase from dengue virus. J Virol. 2008;82(1):173-83.
37. Humphrey W, Dalke A, Schulten K. VMD: Visual molecular dynamics. J Molecular Graphics. 1996;14(1):33-8.
38. Harrach MF, Drossel B. Structure and dynamics of TIP3P, TIP4P, and TIP5P water near smooth and atomistic walls of different hydroaffinity. J Chem Phys. 2014;140(17):174501.
39. Phillips JC, Braun R, Wang W, Gumbart J, Tajkhorshid E, Villa E, et al. Scalable molecular dynamics with NAMD. J Comput Chem. 2005;26(16):1781-802.
40. Best RB, Zhu X, Shim J, Lopes PE, Mittal J, Feig M, et al. Optimization of the additive CHARMM all-atom protein force field targeting improved sampling of the backbone phi, psi and side-chain chi(1) and chi(2) dihedral angles. J Chem Theory Comput. 2012;8(9):3257-73.
41. Darden T, York D, L P. Particle mesh Ewald: An N·log(N) method for Ewald sums in large systems. J Chem Phys. 1993;98:10089-92.
42. Vajda S, Yueh C, Beglov D, Bohnuud T, Mottarella SE, Xia B, et al. New additions to the ClusPro server motivated by CAPRI. Proteins. 2017;85(3):435-44.
43. Kozakov D, Hall DR, Xia B, Porter KA, Padhorny D, Yueh C, et al. The ClusPro web server for protein-protein docking. Nat Protoc. 2017;12(2):255-78.
44. Kozakov D, Beglov D, Bohnuud T, Mottarella SE, Xia B, Hall DR, et al. How good is automated protein docking? Proteins. 2013;81(12):2159-66.
45. Alder BJ, Wainwright TE. Studies in Molecular Dynamics. I. General Method. J Chem Phys. 959;31:459-66.
46. Wang Y, Zheng QC, Kong CP, Tian Y, Zhan J, Zhang JL, et al. Heparin makes differences: a molecular dynamics simulation study on the human betaII-tryptase monomer. Mol Biosyst. 2015;11(1):252-61.
47. Zhu J, Lv Y, Han X, Xu D, Han W. Understanding the differences of the ligand binding/unbinding pathways between phosphorylated and non-phosphorylated ARH1 using molecular dynamics simulations. Sci Rep. 2017;7(1):12439.

48. Trott O, Olson AJ. AutoDock Vina: improving the speed and accuracy of docking with a new scoring function, efficient optimization, and multithreading. J Comput Chem. 2010;31(2):455-61.
49. Dallakyan S, Olson AJ. Small-molecule library screening by docking with PyRx. Methods Mol Biol. 2015;1263:243-50.
50. Pettersen EF, Goddard TD, Huang CC, Couch GS, Greenblatt DM, Meng EC, et al. UCSF Chimera--a visualization system for exploratory research and analysis. J Comput Chem. 2004;25(13):1605-12.
51. Takahashi H, Takahashi C, Moreland NJ, Chang YT, Sawasaki T, Ryo A, et al. Establishment of a robust dengue virus NS3-NS5 binding assay for identification of protein-protein interaction inhibitors. Antiviral Res. 2012;96(3):305-14.
52. Yang CC, Hu HS, Wu RH, Wu SH, Lee SJ, Jiaang WT, et al. A novel dengue virus inhibitor, BP13944, discovered by high-throughput screening with dengue virus replicon cells selects for resistance in the viral NS2B/NS3 protease. Antimicrob Agents Chemother. 2014;58(1):110-9.
53. Grant BJ, Rodrigues AP, ElSawy KM, McCammon JA, Caves LS. Bio3d: an R package for the comparative analysis of protein structures. Bioinformatics. 2006;22(21):2695-6.
54. Skjaerven L, Yao XQ, Scarabelli G, Grant BJ. Integrating protein structural dynamics and evolutionary analysis with Bio3D. BMC Bioinformatics. 2014;15:399.
55. Tay MY, Saw WG, Zhao Y, Chan KW, Singh D, Chong Y, et al. The C-terminal 50 amino acid residues of dengue NS3 protein are important for NS3-NS5 interaction and viral replication. J Biol Chem. 2015;290(4):2379-94.
56. Ceballos-Olvera I, Chavez-Salinas S, Medina F, Ludert JE, del Angel RM. JNK phosphorylation, induced during dengue virus infection, is important for viral infection and requires the presence of cholesterol. Virology. 2010;396(1):30-6.
57. Sreekanth GP, Chuncharunee A, Cheunsuchon B, Noisakran S, Yenchitsomanus PT, Limjindaporn T. JNK1/2 inhibitor reduces dengue virus-induced liver injury. Antiviral Res. 2017;141:7-18.
58. Zandi K, Teoh BT, Sam SS, Wong PF, Mustafa MR, Abubakar S. Antiviral activity of four types of bioflavonoid against dengue virus type-2. Virol J. 2011;8:560.
59. Noppakunmongkolchai W, Poyomtip T, Jittawuttipoka T, Luplertlop N, Sakuntabhai A, Chimnaronk S, et al. Inhibition of protein kinase C promotes dengue virus replication. Virol J. 2016;13:35.
60. Chambers TJ, Weir RC, Grakoui A, McCourt DW, Bazan JF, Fletterick RJ, et al. Evidence that the N-terminal domain of nonstructural protein NS3 from yellow fever virus is a serine protease responsible for site-specific cleavages in the viral polyprotein. Proc Natl Acad Sci U S A. 1990;87(22):8898-902.
61. Agnihotri S, Narula R, Joshi K, Rana S, Singh M. In silico modeling of ligand molecule for non structural 3 (NS3) protein target of flaviviruses. Bioinformation. 2012;8(3):123-7.
62. Mukhametov A, Newhouse EI, Aziz NA, Saito JA, Alam M. Allosteric pocket of the dengue virus (serotype 2) NS2B/NS3 protease: In silico ligand screening and molecular dynamics studies of inhibition. J Mol Graph Model. 2014;52:103-13.
63. Chen J, Jiang H, Li F, Hu B, Wang Y, Wang M, et al. Computational insight into dengue virus NS2B-NS3 protease inhibition: A combined ligand- and structure-based approach. Comput Biol Chem. 2018;77:261-71.
64. Velmurugan D, Mythily U, Rao K. Design and docking studies of peptide inhibitors as potential antiviral drugs for dengue virus ns2b/ns3 protease. Protein Pept Lett. 2014;21(8):815-27.
65. Yoshizumi M, Tsuchiya K, Kirima K, Kyaw M, Suzaki Y, Tamaki T. Quercetin inhibits Shc- and phosphatidylinositol 3-kinase-mediated c-Jun N-terminal kinase activation by angiotensin II in cultured rat aortic smooth muscle cells. Mol Pharmacol. 2001;60(4):656-65.